Photoinduced Nonpersistent Radicals as Polarizing Agents for X-Nuclei Dissolution Dynamic Nuclear Polarization

Article · January 2015

CITATIONS
10

READS
77

8 authors, including:

Andrea Capozzi
École Polytechnique Fédérale de Lausanne
25 PUBLICATIONS **209** CITATIONS
SEE PROFILE

Jean-Noël Hyacinthe
Haute école de santé Genève
49 PUBLICATIONS **466** CITATIONS
SEE PROFILE

Tian Cheng
University of Cambridge
30 PUBLICATIONS **333** CITATIONS
SEE PROFILE

Giovanni Boero
École Polytechnique Fédérale de Lausanne
112 PUBLICATIONS **2,027** CITATIONS
SEE PROFILE

THE JOURNAL OF PHYSICAL CHEMISTRY C

Article

pubs.acs.org/JPCC

Photoinduced Nonpersistent Radicals as Polarizing Agents for X-Nuclei Dissolution Dynamic Nuclear Polarization

Andrea Capozzi,*[,†] Jean-Noël Hyacinthe,[∥,⊥] Tian Cheng,[†] Tim R. Eichhorn,[†,#] Giovanni Boero,[‡] Christophe Roussel,[§] Jacques J. van der Klink,[†] and Arnaud Comment*[,†]

[†]Institute of Physics of Biological Systems, [‡]Institute of Microengineering, and [§]Section of Chemistry and Chemical Engineering, Institute of Chemical Sciences and Engineering, EPFL, Lausanne, Switzerland

[∥]School of Health Sciences − Geneva, University of Applied Sciences and Arts Western Switzerland (HES-SO), Geneva, Switzerland

[⊥]Image Guided Interventions Laboratory, Faculty of Medicine, University of Geneva, Geneva, Switzerland

[#]Sample Environment and Polarized Targets Group, PSI, Villigen, Switzerland

Supporting Information

ABSTRACT: Hyperpolarization via dissolution dynamic nuclear polarization (DNP) is a versatile method to dramatically enhance the liquid-state NMR signal of X-nuclei and can be used for performing metabolic and molecular imaging. It was recently demonstrated that instead of incorporating persistent radicals as source of unpaired electron spins, required for DNP, nonpersistent radicals can be photoinduced in frozen beads of neat pyruvic acid (PA), the most common substrate for metabolic imaging. In the present work, it is shown that the same radicals can be created in frozen solutions containing a fraction of PA in addition to ^{13}C- or ^{6}Li-labeled salts or ^{129}Xe nuclei. The use of these nonpersistent radicals prevents the loss of a substantial part of the polarization during the transfer of hyperpolarized solutions into iron-shielded high-field MRI scanners. It is also demonstrated that UV-irradiated d_4-PA yields nonpersistent radicals exhibiting similarities with the most efficient and widely used persistent trityl radicals.

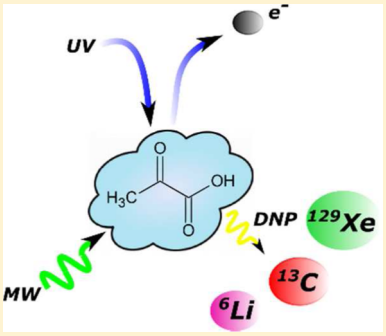

I. INTRODUCTION

Since its development, only slightly more than a decade ago,[1] hyperpolarization via dynamic nuclear polarization (DNP) has rapidly become a well-established and widespread technique for enhancing the nuclear magnetic resonance (NMR) signal of low-gamma nuclei that exhibit long liquid-state longitudinal relaxation time (T_1) such as ^{13}C, ^{6}Li, ^{129}Xe, and ^{15}N.[2−7] The principle of DNP, known from more than half a century,[8] is to embed radicals, which hold unpaired electron spins, within a glassy sample and transfer the high electron spin polarization obtained by both lowering the sample temperature (1−4 K) and applying an external magnetic field of 3.35−7 T to the nuclear spins of the sample. This is done by shining microwaves slightly off-resonance from the center of the electron spin resonance (ESR) line of the radicals. It has been demonstrated that the nuclear spin order achieved by DNP in the solid state can be maintained through a rapid dissolution method producing liquid-state hyperpolarized (HP) solutions.[9] The lifetime of the HP state is however limited by T_1, which is reduced by the presence of the routinely used persistent radicals.[10−13] Moreover, for medical applications, the radicals need to be removed from the final HP solutions prior to injection. An alternative to filtering or artificial scavenging of the paramagnetic impurities[14,15] would be to use nonpersistent radicals that are stable at low temperature but recombine during the dissolution step. It was recently shown that such radicals can be produced in concentrations suitable for performing DNP by means of low-temperature (77 K) UV-irradiation of neat pyruvic acid (PA) frozen beads.[16] The original work also reported that the nonpersistent radicals can be induced in water:PA 1:1 (v/v) mixtures. In this article, we extend this method and demonstrate that other compounds besides PA can be hyperpolarized using these photoinduced nonpersistent radicals.

II. EXPERIMENTAL METHODS

a. Samples Preparation. *ESR Samples.* By means of a micropipet (1−20 μL range), three 8.0 ± 0.5 μL drops of neat or diluted (in H_2O, ethanol, or THF) PA or its deuterated form (d_4-PA) were poured, one by one, inside a synthetic quartz dewar (Wilmad, 150 mL Suprasil dewar flask type WG-850-B-Q) filled with liquid nitrogen. Samples were irradiated for up to 70 min (turning the dewar of 90° every 10 min) using a 1024 mW maximum output power 365 nm LED array (Hamamatsu LC-L5). Once the irradiation process was completed, the dewar was inserted into the ESR spectrometer cavity for measurements.

Received: July 29, 2015
Revised: September 8, 2015
Published: September 8, 2015

DOI: 10.1021/acs.jpcc.5b07315
J. Phys. Chem. C 2015, 119, 22632−22639

Carbon DNP Samples. 2.25 M sodium [1-^{13}C]acetate solutions were prepared in H_2O:ethanol 1:1 (v/v) before adding an amount of PA or d_4-PA corresponding to 30% of the total volume to obtain a final 1.5 M acetate concentration. The UV-irradiation procedure was performed as described above for 1 h on about 25 frozen beads (~200 μL of solution). An additional sample containing nitroxyl radicals as paramagnetic centers was prepared by adding 50 mM of TEMPOL to a H_2O:ethanol 1:1 (v/v) solution containing 1.5 M sodium [1-^{13}C]acetate.

Xenon DNP Samples. Following methods already described in an earlier publication,[5] liquid xenon was embedded in a 2-methyl-1-pentanol:PA (or d_4-PA) mixture (with the acid corresponding to 10% of the final volume) to yield 5 M xenon samples. Once frozen in liquid nitrogen, the samples were extracted from the coldfinger and placed into the quartz dewar filled with liquid nitrogen in order to perform 1 h of UV-irradiation.

Lithium DNP Samples. 4.5 M ^{6}LiCl solutions were prepared in H_2O:ethanol 1:1 (v/v) before adding an amount of PA corresponding to 30% of the total volume to obtain a final 3 M lithium concentration. About 200 μL of sample (25 frozen beads) were irradiated at low temperature with UV light for 1 h.

Natural abundance xenon gas was purchased from Carbagas, Lausanne, Switzerland; all the other chemicals were obtained from Sigma-Aldrich, Buchs, Switzerland.

b. Low-Temperature X-Band ESR Methods. An X-band spectrometer (EMX, Bruker Biospin, Rheinstetten, Germany) was used for all ESR experiments. The tail of the quartz dewar, filled with liquid nitrogen, was placed inside the resonator cavity of the spectrometer. A series of reference ESR signals arising from three 8.0 ± 0.5 μL frozen beads of ethanol containing TEMPO (2,2,6,6-tetramethylpiperidoxyl) radical at various known concentrations (between 25 and 100 mM) were used to calibrate the radical concentration as a function of signal integral (see Supporting Information Figure S1). The same parameters were kept for all ESR measurements, i.e., center of the magnetic field sweep: 338 mT; sweep range: 30 mT; sweep time: 20 s; modulation frequency: 6 kHz; modulation amplitude: 2 G; microwave output power: 0.063 mW. Parameters were optimized in order to work in the linear range of the detector diode of the ESR spectrometer and to avoid spurious line-broadening effects.

c. Sample Transfer into the DNP Polarizer. Once the low-temperature UV-irradiation was completed, the frozen beads were quickly transferred from the coldfinger into a polystyrene box containing liquid nitrogen. Afterward, the handling of the sample was standard: a polytetrafluoroethylene (PTFE) sample cup was precooled in liquid nitrogen, and the beads were placed inside the cup before it was rapidly inserted into the cryostat prefilled with liquid helium (see ref 20 for details). The handling of the sample is not problematic since the radicals are stable at liquid nitrogen temperature (77 K). A precise evaluation of their temporal degradation as a function of temperature has however not yet been performed. It must nevertheless be noted that it was possible to perform DNP experiments on irradiated samples stored for months in liquid nitrogen without observing consistent differences in maximum ^{13}C polarization or build-up time constant compared to samples prepared the same day.

d. Solid-State and Liquid-State DNP Methods. Solid-state DNP measurements were performed using two different custom-built polarizers: one operating at 5 T and coupled to a 14.1 T rodent MRI scanner (Varian, USA)[17] and the other operating at 7 T and coupled to a 9.4 T rodent MRI scanner (Varian, USA).[18,19] The 5 T polarizer was used for the ^{13}C and ^{129}Xe DNP experiments whereas the ^{6}Li DNP experiments were performed using the 7 T polarizer.

Samples containing sodium [1-^{13}C]acetate were polarized at 1.50 ± 0.05 and 1.15 ± 0.05 K by shining microwaves at a frequency ranging from 139.50 to 140.50 GHz with a nominal output power of 55 mW (ELVA-1, St. Petersburg, Russia). The ^{13}C polarization time evolution was monitored using a homemade NMR setup,[20] applying a 2° radio-frequency (rf) pulse at 53.437 MHz every 5 min. Once the maximum polarization was reached, a 20° rf pulse was applied, and once the microwaves were switched off and after waiting for a sufficiently long time for complete relaxation of the sample nuclear spin magnetization, an identical 20° rf pulse was applied to measure the reference signal corresponding to the nuclear Boltzmann polarization. The DNP enhancement was obtained by computing the ratio between the two NMR signal integrals. Once polarized, the samples were dissolved and automatically transferred into an injection pump (equipped with a rf probe tuned at 150.25 MHz) located inside a nonactively shielded 14.1 T rodent MRI scanner. The setup and procedures were similar to the previously described ones,[19,20] with the notable differences that the length of the plastic tube for the transfer of the HP solution was 10 m instead of 5 m and the solution transfer time was set to 5 s instead of 2 s.

The ^{1}H NMR signal was recorded as well while polarizing the [1-^{13}C]acetate samples. The ^{1}H signal evolution and DNP enhancement were measured as described above, with the difference that the NMR hardware components (coil, filter, and power amplifier) were adapted to 212.5 MHz and the bottom of the inset supporting the sample was entirely made of PTFE to avoid any signal contamination from surrounding protons.

Samples containing ^{129}Xe were polarized at 1.50 ± 0.05 K by shining microwaves at a frequency corresponding to the optimal DNP conditions for each radical (139.875 GHz for UV-irradiated PA, 139.925 GHz for UV-irradiated d_4-PA, and 140.3 GHz for TEMPOL; see Supporting Information). The ^{129}Xe polarization time evolution and DNP enhancement were measured using a procedure identical to the one used for the ^{13}C experiments, with the difference that the NMR frequency was set to 58.787 MHz.

The ^{6}Li samples were polarized at 1.50 ± 0.05 K in the 7 T DNP setup. The microwave frequency was set to the value corresponding to the maximum DNP enhancement (196.75 GHz; see Supporting Information) and the nominal output power was 55 mW (ELVA-1, St. Petersburg, Russia). The ^{6}Li polarization time evolution was monitored, using a homemade NMR setup, by applying a 5° rf pulse at 43.973 MHz every 5 min. Because of the prohibitively long T_1, the solid-state ^{6}Li DNP enhancement was not evaluated. Once dissolved, the ^{6}Li T_1 and maximum liquid-state polarization were evaluated using a rf probe (tuned at 58.89 MHz) located around a custom-made injection pump, as described in a previous publication.[18−20] The HP ^{6}Li signal decay was monitored by applying a 10° rf pulse every 10 s. The thermally polarized NMR signal was measured using the same 10° pulse (16 averages with a repetition time TR = $5T_1$). The DNP enhancement was obtained by computing the ratio between the signal integral of the first measured spectrum and the thermally polarized spectrum.

DOI: 10.1021/acs.jpcc.5b07315
J. Phys. Chem. C 2015, 119, 22632−22639

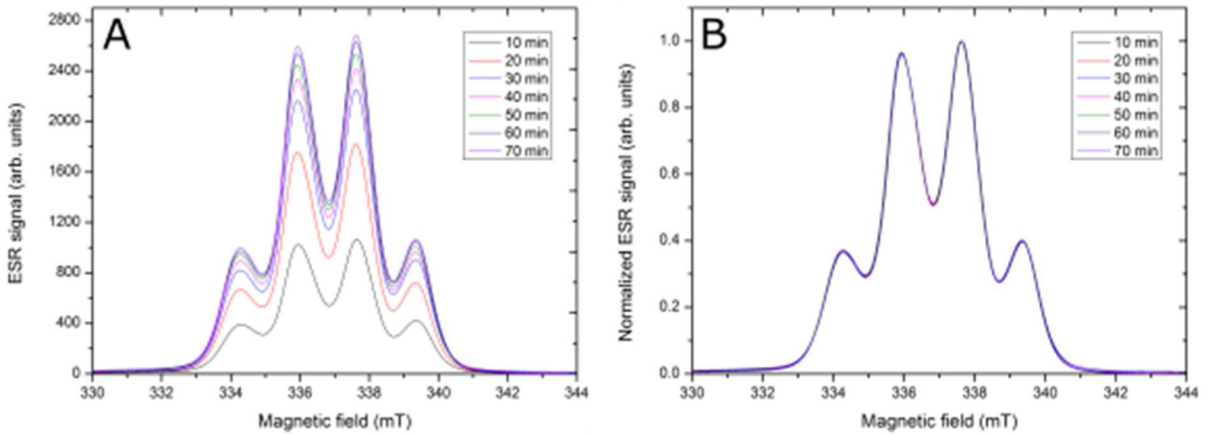

Figure 1. Integrated X-band spectrum of UV-irradiated neat PA measured at 77 K as a function of the irradiation time in arbitrary units (A) and normalized to 1 (B).

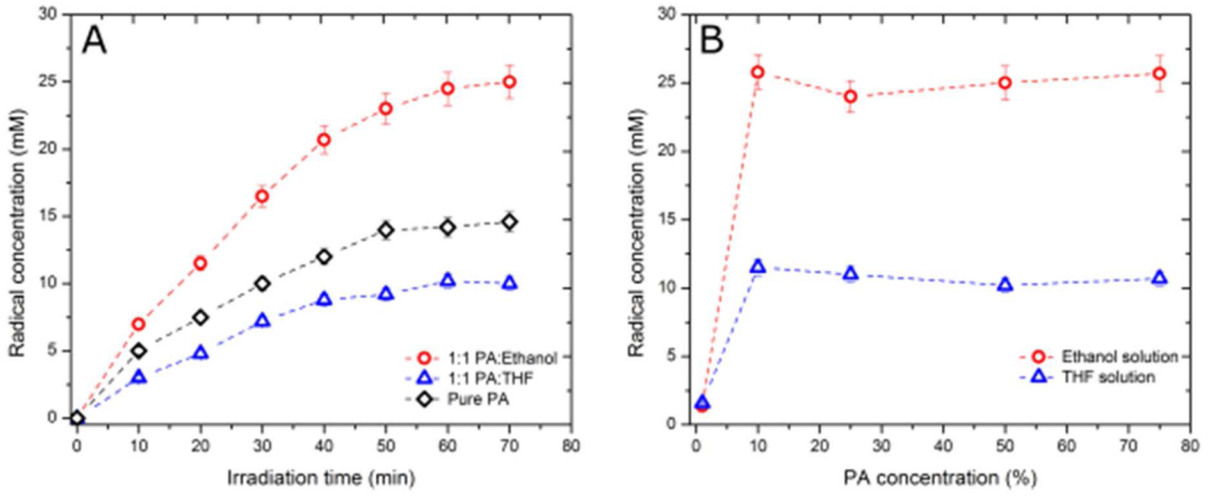

Figure 2. (A) Radical concentration generated by low-temperature (77 K) UV-irradiation as a function of the illumination time for frozen beads of neat PA (black diamonds), PA:ethanol 1:1 (v/v) (red circles), and PA:THF 1:1 (v/v). (B) Radical concentration generated after 60 min low-temperature (77 K) UV-irradiation as a function of the PA concentration in the frozen beads of ethanol (red circles) and THF (blue triangles) solutions. Dashed lines serve as guide for the eyes.

III. RESULTS AND DISCUSSION

Similar X-band ESR spectra were obtained for all UV-irradiated samples, independently of their composition, suggesting that the signal arises from an electron located on a PA molecular orbital. Moreover, it was observed that the broadening of the spectral line width is independent of the radical concentration. A representative example is reported for neat PA in Figure 1 where ESR spectra measured at 77 K as a function of UV-irradiation time are presented. A spectrum was measured after each consecutive 10 min of UV-irradiation and reported in arbitrary units (panel A) and normalized to 1 (panel B). The comparison between panels A and B clearly demonstrates that the line shape is independent of the radical concentration.

Although the nature of the generated radicals is solvent-independent (see Figure S2), the solvent plays a role in the radical yield. The radical concentration as a function of the UV-irradiation time is shown in Figure 2A for neat PA, PA:ethanol 1:1 (v/v), and PA:THF 1:1 (v/v) frozen beads. In all cases, a plateau was reached after about 1 h of UV-irradiation. Tentatively, we suggest that a polar solvent such as ethanol (H_2O relative polarity = 0.654)[21] increases the radical yield (25.0 ± 1.5 mM) compared to neat PA (15.0 ± 0.7 mM), while a less polar one such as THF (H_2O relative polarity = 0.207)[21] diminishes it (9.0 ± 0.5 mM). Samples prepared by diluting PA in equal volume with water (27.0 ± 1.5 mM of radical concentration after 1 h UV-irradiation) exhibited a behavior similar to the samples containing ethanol.[16]

A central point for DNP applications is the determination of the minimum PA to solvent ratio necessary to obtain a sufficient radical concentration following UV-irradiation, in particular if PA is not the target substrate to be hyperpolarized. To elucidate this point, the radical concentration was measured, after 1 h of UV-irradiation, as a function of the PA dilution in ethanol and THF solutions (Figure 2B). For both solvents, it was observed that the radical concentration is independent of the PA dilution for any PA concentration above 10% of the total volume, corresponding to a minimum of 1.4 M. A dramatic reduction of the radical concentration was however observed in solutions containing only 1% of PA (0.14 M).

In addition to UV-irradiated natural abundance PA, it is also herein proposed to use UV-irradiated d_4-PA as DNP polarizing agent because it has been shown that narrower ESR line radicals lead to higher ^{13}C polarization.[22] The integrated X-band ESR spectrum of UV-irradiated frozen beads of neat PA

DOI: 10.1021/acs.jpcc.5b07315
J. Phys. Chem. C 2015, 119, 22632−22639

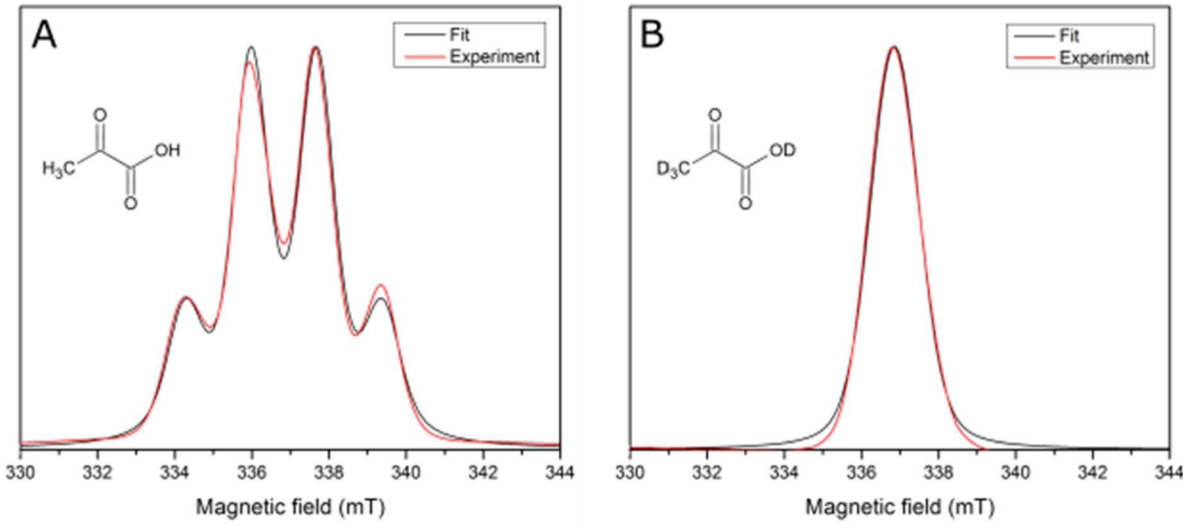

Figure 3. (A) Integrated X-band ESR spectrum of UV-irradiated neat natural abundance PA measured at 77 K in 8.0 ± 0.5 μL frozen beads after 60 min UV-irradiation. Inset: structural formula of natural abundance PA. (B) Integrated X-band ESR spectrum of UV-irradiated neat d_4-PA measured at 77 K in 8.0 ± 0.5 μL frozen beads after 60 min UV-irradiation. Inset: structural formula of d_4-PA.

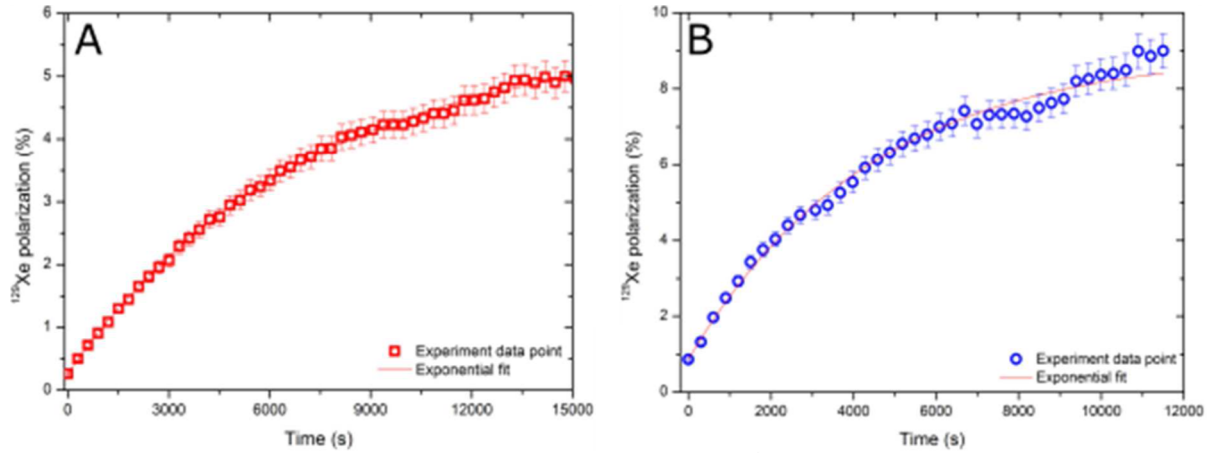

Figure 4. Solid-state ^{129}Xe polarization build-up curves measured at 5 T and 1.5 K in 5 M xenon samples prepared in (A) a 2-methyl-1-pentanol/PA mixture (10% of PA in the final volume) and (B) a 2-methyl-1-pentanol/d_4-PA mixture (10% of d_4-PA in the final volume).

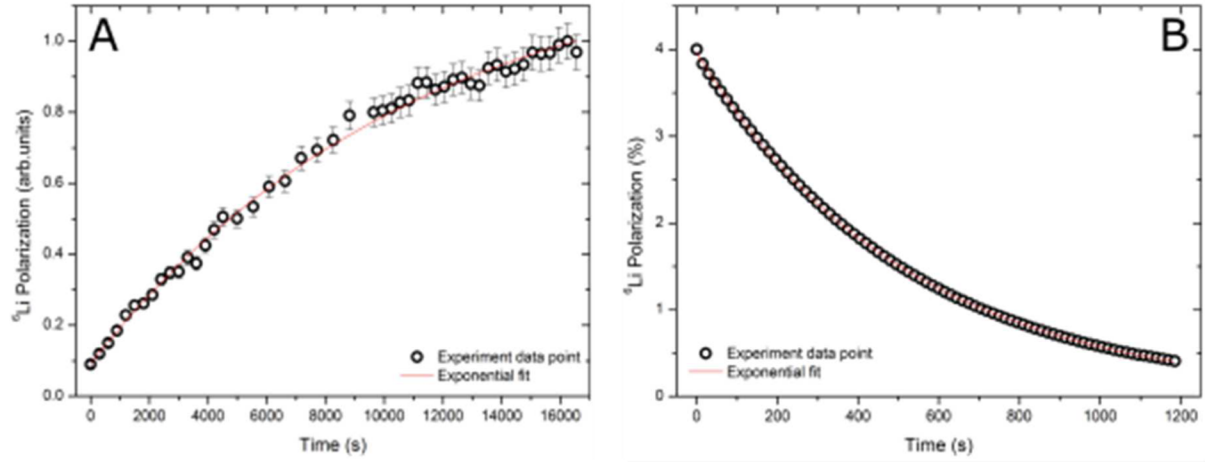

Figure 5. (A) Solid-state ^{6}Li DNP build-up curve measured at 7 T and 1.5 K in a 3 M ^{6}LiCl sample prepared in H_2O:ethanol 1:1 (v/v) with 30% UV-irradiated PA. (B) Liquid-state ^{6}Li signal decay measured in an injection pump placed inside a 9.4 T rodent MRI scanner.

and d_4-PA are shown in Figure 3. Experimental data were fitted using the PEPPER routine of the MATLAB-based software EASYSPIN,[23] considering a spin 1/2 radical with isotropic hyperfine coupling to the methyl protons or deuterons for

DOI: 10.1021/acs.jpcc.5b07315
J. Phys. Chem. C 2015, 119, 22632−22639

natural abundance or deuterated PA, respectively. We deduced that PA and d_4-PA have the same **g**-tensor and dipolar broadening but that irradiated d_4-PA has a 6.57-fold smaller hyperfine coupling constant than its protonated counterpart (see Supporting Information). This is in good agreement with the proportion between ^{1}H and ^{2}H gyromagnetic ratios (γ_{1H}/γ_{2H} = 6.51).[24] Moreover, as expected, the radical yield was identical for both PA and d_4-PA (16.0 ± 1.0 mM after 1 h of UV-irradiation).

In the following, we report experimental results demonstrating that UV-irradiated PA and d_4-PA can be used as efficient polarizing agent for enhancing the polarization of ^{129}Xe as well as ^{6}Li and ^{13}C in LiCl and sodium [1-^{13}C]acetate frozen solutions, respectively. As already mentioned, ^{129}Xe DNP experiments were performed at 5 T and 1.5 K.[17] A solid-state ^{129}Xe polarization of 5.0 ± 0.2% was measured after 3 h, about 1.5 times higher than what was obtained using nitroxyl radicals as polarizing agent.[5] A representative ^{129}Xe polarization build-up curve is shown in Figure 4A.

The lithium sample was polarized for 5 h at 1.5 K in our original (now set to 7 T) polarizer and subsequently dissolved prior to transfer into the 9.4 T rodent MRI scanner (Varian/Magnex, Palo Alto, CA) coupled to the polarizer.[18] A liquid-state polarization of 4.0 ± 0.5% was measured in the infusion pump placed inside the scanner bore following the protocol described in a former publication.[19] Even though the polarization value was lower than what is reported in the literature for samples prepared with nitroxyl radicals,[4] a remarkably long relaxation time of 519 ± 25 s was determined, equivalent to the room-temperature ^{6}Li T_1 measured in thermally polarized ^{6}LiCl aqueous solutions at 9.4 T.[25] Results are reported in Figure 5.

To investigate in more details the DNP properties of the UV-induced radicals, sodium [1-^{13}C]acetate samples were studied. Our analysis relies on the measurement of the ^{1}H and ^{13}C DNP microwave spectra performed for the three samples (Figure 6). The sample containing TEMPOL (Figure 6A) exhibits an essentially identical spectrum for both nuclei, similar to what has been found for the nitroxyl radical porphyrexide.[26] At each irradiation frequency, both ^{1}H and ^{13}C reach the same spin temperature in the stationary state (and it is expected that *all* nuclei would do the same). This is very different from the behavior observed with trityl radicals.[9] The types of radicals leading to identical microwave spectra for all nuclei are usually referred to as "broad-line" radicals whereas the others are called "narrow-line" radicals. In a comparative study of five radicals, it was found that replacement of protons in the solvent by deuterons leads to a 2- or 3-fold improvement of ^{13}C−DNP for "broad-line" radicals, while the reverse effect was found for "narrow-line" radicals.[12] It has also been demonstrated in aqueous sodium [1-^{13}C]acetate samples doped with TEMPO that both proton and ^{13}C spin temperatures decrease and remain essentially identical to one another with increasing degree of deuteration.[2] As a consequence, the composition of the sample presented in Figure 6A is not optimal for a "broad-line" radical, and a doubling of the enhancement is expected upon deuteration. Further improvement could also be obtained by optimizing the water/ethanol ratio as well as the radical concentration and by increasing the acetate concentration.[2] The choice of a protonated matrix for the present measurements was made to allow a fair comparison, based on the physical DNP mechanism, between radicals with different ESR line width.

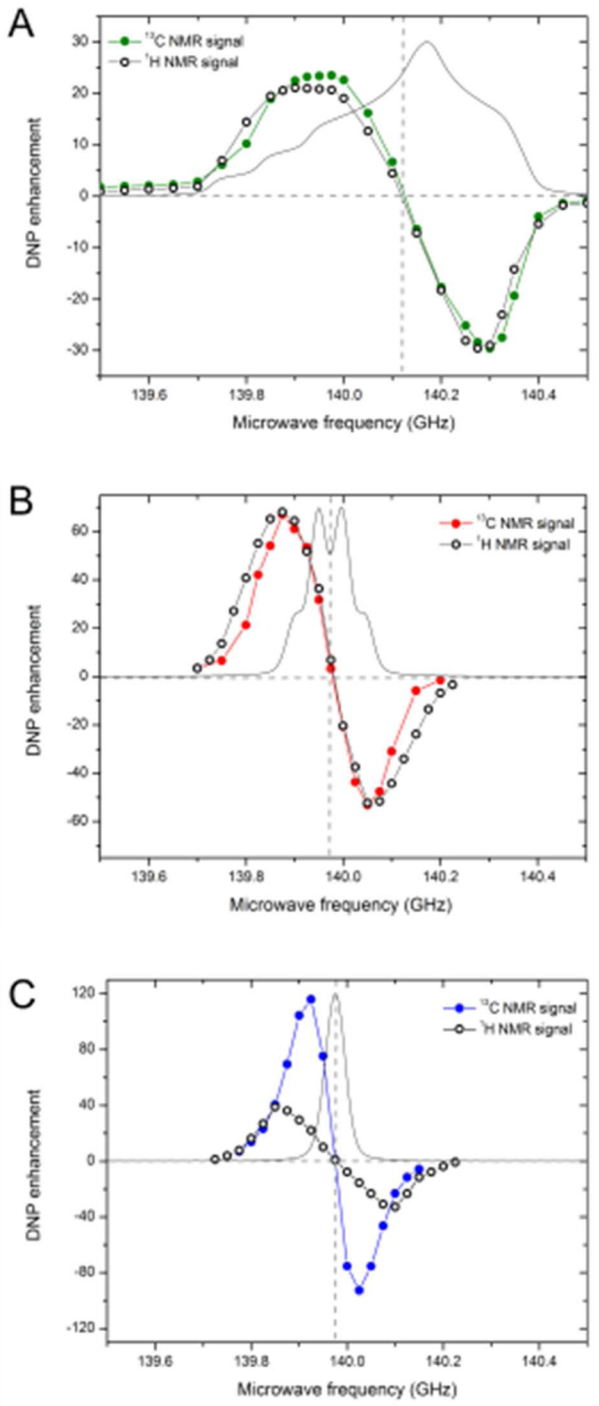

Figure 6. ^{13}C and ^{1}H DNP microwave spectra measured at 5 T and 1.5 K in 1.5 M sodium [1-^{13}C]acetate samples prepared in water:ethanol 1:1 (v/v) mixtures containing TEMPOL (A), UV-irradiated PA (B), or UV-irradiated d_4-PA (C). The simulated ESR spectrum for each of the three radical types is superimposed (solid gray lines). The vertical gray dashed lines represent the center of gravity of the ESR spectra.

The ^{1}H microwave spectrum shown in Figure 6B is slightly broader than the corresponding ^{13}C spectrum, but the DNP maxima appear at the same frequencies for both nuclei. It is therefore likely that the type of radicals present in this sample exhibits a "broad-line" behavior, for which deuteration could improve the maximum ^{13}C polarization. From a theoretical

DOI: 10.1021/acs.jpcc.5b07315
J. Phys. Chem. C 2015, 119, 22632−22639

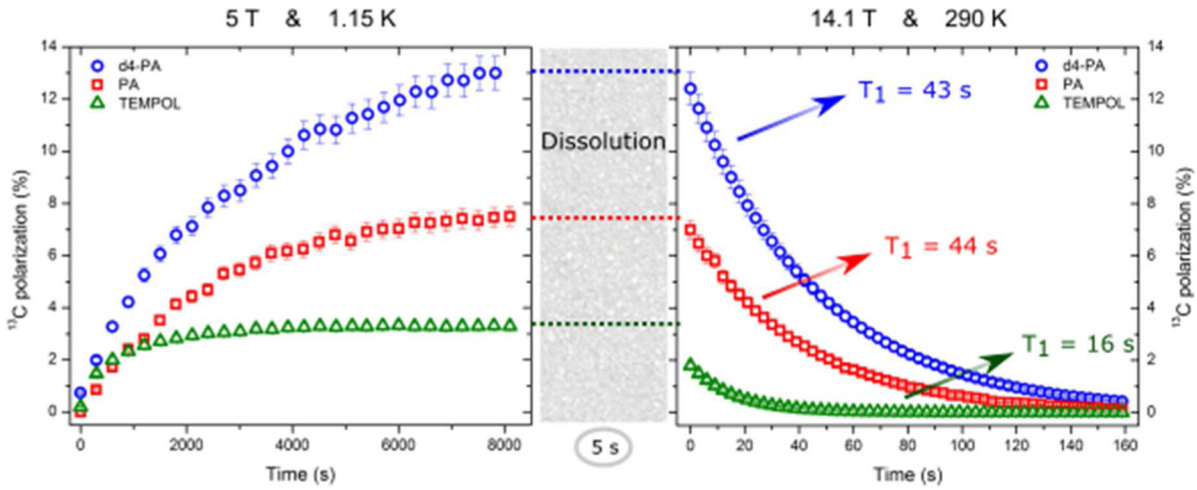

Figure 7. ^{13}C DNP build-up curves recorded in a 5 T/1.15 K polarizer (left panel) and room-temperature relaxation curves measured, after dissolution and transfer, in an injection pump placed inside a 14.1 T MR scanner (right panel). The samples consisted in frozen 1.5 M sodium [1-^{13}C]acetate samples prepared in water/ethanol mixtures containing UV-irradiated PA (red squares), UV-irradiated d_4-PA (blue circles), or TEMPOL (green triangles). Colored dashed lines prolong the NMR signal obtained at the end of the DNP process to visually underline the polarization losses during the transfer; arrows in the right panel indicate the measured ^{13}C T_1 of each sample in the 14.1 T MR scanner.

standpoint, the sample corresponding to Figure 6C is the most interesting. Compared to what was shown in refs 9 and 26, this is an intermediate case for which the two microwave spectra are clearly distinct, although the proton spectrum is not well resolved. The ratio between the largest ^{1}H and ^{13}C enhancements is about 3, which is smaller than the one reported in ref 9 for trityl radicals. At the frequencies corresponding to the extrema of the ^{13}C microwave spectrum of Figure 6C, the ^{1}H enhancement is rather low because most of the "cooling power" delivered by the microwaves is spent on polarizing the low-gamma nuclei, in particular ^{13}C. In this case, deuteration is not expected to improve the ^{13}C polarization. The difference in ^{13}C enhancement between the samples of Figure 6B,C are most likely linked to the two competing effects highlighted in ref 12. A similar behavior was found for ^{129}Xe when the UV-irradiated d_4-PA radical was used: instead of the 5.0 ± 0.2% polarization mentioned above for the protonated radical, a value of 9.5 ± 0.4% was recorded with its deuterated form (see Figure 4B). It is therefore expected that all low-gamma nuclei will follow this trend.

The acetate samples were also used for investigating one crucial point of the dissolution-DNP technique: the transfer of the HP solution from the polarizer to the NMR/MRI system. To minimize the transfer time, the dissolved sample can be driven through a plastic tube from one instrument to the other using compressed He gas.[1,9,20,27] An ill-defined combination of several liquid-state relaxation mechanisms may cause loss of polarization along the way and it is generally believed that the path should not pass through regions of very low or very rapidly changing magnetic field values (the so-called adiabatic condition). The above-mentioned issue has been recently studied in some details for ^{1}H and ^{13}C.[28] As the UV-induced radicals are entirely quenched when the temperature of the sample is raised during the dissolution process, there is a disappearance of the main relaxation mechanism causing nuclear polarization losses, namely paramagnetic relaxation.

In the herein reported hyperpolarized ^{13}C experiments, the HP solution was transferred into the bore of a nonactively shielded 14.1 T rodent MRI scanner (Varian/Magnex, Palo Alto, CA) from the polarizer located outside of the massive iron shielding structure of the scanner. The ^{13}C polarization build-up measured in the 5 T/1.15 K polarizer is displayed in the left-hand panel of Figure 7 (the microwave frequency was set to the optimal frequency determined by the ^{13}C microwave spectrum shown in Figure 6). The central panel of the figure pictures the unknown fate of the polarization during the 5 s that it takes to transfer the solution from the polarizer into the infusion pump placed inside the 14.1 T scanner bore,[20] where the acetate liquid-state ^{13}C polarization decay was monitored (Figure 4, right panel).[19] The essential result is that the polarization created by the two nonpersistent radicals was almost entirely maintained throughout the transfer across the complex field path between the polarizer and the scanner (about 5% relative difference between solid-state and liquid-state ^{13}C polarization); conversely, the sample containing TEMPOL suffered a clear polarization loss of around half of its solid-state value. A correlation is that the acetate liquid-state ^{13}C T_1 measured in the 14.1 T scanner for the sample containing nitroxyl radicals is much shorter (16.2 ± 0.1 s) than for the other two samples in which the UV-induced radicals quenched at the time of dissolution. The dissolved UV-irradiated samples indeed exhibited a T_1 value nearly identical to the value measured for melted nonirradiated PA beads in a 600 MHz high-resolution system (45 ± 1 s).

IV. CONCLUSIONS

The herein presented results demonstrate that radicals created by UV-irradiation of PA exemplify a low-cost and versatile way for polarizing X-nuclei in molecules that can be codissolved, together with a fraction of PA, in a medium with a polarity comparable to that of water. Moreover, the self-quenching property of these radicals upon dissolution offers a promising solution for simplifying the HP liquid transfer procedure from the polarizer to a high-field MRI scanner with minimal polarization losses. An additional advantage of the automatic elimination of the potentially toxic radical species during dissolution could in principle be to alleviate the quality control procedure required in human MRI/MRS.

Even though at the present stage of the work the radical concentration obtained after UV-irradiation of PA is still rather

DOI: 10.1021/acs.jpcc.5b07315
J. Phys. Chem. C 2015, 119, 22632−22639

low to efficiently perform DNP at high magnetic field, other biocompatible solvent systems are under investigation to improve the radical yield. Furthermore, we are directing our efforts in the research or synthesis of new molecules with the same photochemical properties than PA, but with a more isolated molecular environment at the site of the unpaired electron. A reduced hyperfine coupling between the latter and surrounding nuclei would produce a sharper EPR-line radical species. Increasing the radical yield, or even the discovery of other UV-induced radicals, will provide a more generic improvement of the method for a widespread use of nonpersistent radicals for DNP. Concerning the practical applications of this method, it is important to note that the liquid-state measurements were performed inside an injection pump designed for *in vivo* rodent experiments, meaning that all liquid-state values reported for ^{13}C and ^{6}Li nuclei correspond to the polarization levels at the time of injection, and although these values are not the highest obtained to date, they are sufficient for performing *in vivo* studies with the competitive advantage that the solutions are free of radicals.[16]

■ ASSOCIATED CONTENT

Supporting Information

The Supporting Information is available free of charge on the ACS Publications website at DOI: 10.1021/acs.jpcc.5b07315.

X-band ESR spectrometer calibration curve; ESR additional data and fitting parameters; ^{129}Xe and ^{6}Li DNP microwaves spectra (PDF)

■ AUTHOR INFORMATION

Corresponding Authors

*E-mail andrea.capozzi@epfl.ch.
*E-mail arnaud.comment@epfl.ch.

Notes

The authors declare no competing financial interest.

■ ACKNOWLEDGMENTS

We thank Dr. Ben van den Brandt and Dr. Patrick Hautle who kindly helped us with the X-band ESR measurements at PSI. Our acknowledgment goes also to Dr. Gil Navon and Dr. Mor Mishkovsky for their suggestions about ^{6}Li experiments. We also thank Dr. Hikari Yoshihara for the constructive discussions about the nature of the UV-radical. This work was supported by the Swiss National Science Foundation (Grant PP00P2_157547), the Centre d'Imagerie BioMédicale (CIBM) of the UNIL, UNIGE, HUG, CHUV, EPFL, the Leenards and Jeantet Foundations and a SOCLE grant of the School of Health Sciences − Geneva, University of Applied Sciences and Arts Western Switzerland.

■ REFERENCES

(1) Ardenkjaer-Larsen, J. H.; Fridlund, B.; Gram, A.; Hansson, G.; Hansson, L.; Lerche, M. H.; Servin, R.; Thaning, M.; Golman, K. Increase in Signal-to-Noise Ratio of > 10,000 Times in Liquid-State Nmr. *Proc. Natl. Acad. Sci. U. S. A.* **2003**, *100*, 10158−10163.

(2) Kurdzesau, F.; van den Brandt, B.; Comment, A.; Hautle, P.; Jannin, S.; van der Klink, J. J.; Konter, J. A. Dynamic Nuclear Polarization of Small Labelled Molecules in Frozen Water-Alcohol Solutions. *J. Phys. D: Appl. Phys.* **2008**, *41*, 155506 1−10.

(3) Cudalbu, C.; Comment, A.; Kurdzesau, F.; van Heeswijk, R. B.; Uffmann, K.; Jannin, S.; Denisov, V.; Kirik, D.; Gruetter, R. Feasibility of in Vivo N-15 Mrs Detection of Hyperpolarized N-15 Labeled Choline in Rats. *Phys. Chem. Chem. Phys.* **2010**, *12*, 5818−5823.

(4) van Heeswijk, R. B.; et al. Hyperpolarized Lithium-6 as a Sensor of Nanomolar Contrast Agents. *Magn. Reson. Med.* **2009**, *61*, 1489−1493.

(5) Capozzi, A.; Roussel, C.; Comment, A.; Hyacinthe, J. N. Optimal Glass-Forming Solvent Brings Sublimation Dynamic Nuclear Polarization to Xe-129 Hyperpolarization Biomedical Imaging Standards. *J. Phys. Chem. C* **2015**, *119*, 5020−5025.

(6) Comment, A.; et al. Hyperpolarizing Gases Via Dynamic Nuclear Polarization and Sublimation. *Phys. Rev. Lett.* **2010**, *105*, 8104 1−4.

(7) Karlsson, M.; Jensen, P. R.; Duus, J. O.; Meier, S.; Lerche, M. H. Development of Dissolution Dnp-Mr Substrates for Metabolic Research. *Appl. Magn. Reson.* **2012**, *43*, 223−236.

(8) Abragam, A.; Goldman, M. Principles of Dynamic Nuclear-Polarization. *Rep. Prog. Phys.* **1978**, *41*, 395−467.

(9) Wolber, J.; et al. Generating Highly Polarized Nuclear Spins in Solution Using Dynamic Nuclear Polarization. *Nucl. Instrum. Methods Phys. Res., Sect. A* **2004**, *526*, 173−181.

(10) Lumata, L.; Merritt, M.; Khemtong, C.; Ratnakar, S. J.; van Tol, J.; Yu, L.; Song, L. K.; Kovacs, Z. The Efficiency of Dpph as a Polarising Agent for Dnp-Nmr Spectroscopy. *RSC Adv.* **2012**, *2*, 12812−12817.

(11) Lumata, L.; Merritt, M. E.; Malloy, C. R.; Sherry, A. D.; Kovacs, Z. Impact of Gd3+ on Dnp of [1-C-13]Pyruvate Doped with Trityl Ox063, Bdpa, or 4-Oxo-Tempo. *J. Phys. Chem. A* **2012**, *116*, 5129−5138.

(12) Lumata, L.; Merritt, M. E.; Kovacs, Z. Influence of Deuteration in the Glassing Matrix on C-13 Dynamic Nuclear Polarization. *Phys. Chem. Chem. Phys.* **2013**, *15*, 7032−7035.

(13) Lumata, L.; Ratnakar, S. J.; Jindal, A.; Merritt, M.; Comment, A.; Malloy, C.; Sherry, A. D.; Kovacs, Z. Bdpa: An Efficient Polarizing Agent for Fast Dissolution Dynamic Nuclear Polarization Nmr Spectroscopy. *Chem. - Eur. J.* **2011**, *17*, 10825−10827.

(14) Nelson, S. J.; et al. Metabolic Imaging of Patients with Prostate Cancer Using Hyperpolarized [1-C-13]Pyruvate. *Sci. Transl. Med.* **2013**, *5*, 198ra108 1−10.

(15) Mieville, P.; et al. Scavenging Free Radicals to Preserve Enhancement and Extend Relaxation Times in Nmr Using Dynamic Nuclear Polarization. *Angew. Chem., Int. Ed.* **2010**, *49*, 6182−6185.

(16) Eichhorn, T. R.; Takado, Y.; Salameh, N.; Capozzi, A.; Cheng, T.; Hyacinthe, J. N.; Mishkovsky, M.; Roussel, C.; Comment, A. Hyperpolarization without Persistent Radicals for in Vivo Real-Time Metabolic Imaging. *Proc. Natl. Acad. Sci. U. S. A.* **2013**, *110*, 18064−18069.

(17) Jannin, S.; Comment, A.; Kurdzesau, F.; Konter, J. A.; Hautle, P.; van den Brandt, B.; van der Klink, J. J. A 140 Ghz Prepolarizer for Dissolution Dynamic Nuclear Polarization. *J. Chem. Phys.* **2008**, *128*, 241102 1−4.

(18) Cheng, T.; Capozzi, A.; Takado, Y.; Balzan, R.; Comment, A. Over 35% Liquid-State C-13 Polarization Obtained Via Dissolution Dynamic Nuclear Polarization at 7 T and 1 K Using Ubiquitous Nitroxyl Radicals. *Phys. Chem. Chem. Phys.* **2013**, *15*, 20819−20822.

(19) Cheng, T.; Mishkovsky, M.; Bastiaansen, J. A. M.; Ouari, O.; Hautle, P.; Tordo, P.; van den Brandt, B.; Comment, A. Automated Transfer and Injection of Hyperpolarized Molecules with Polarization Measurement Prior to in Vivo Nmr. *NMR Biomed.* **2013**, *26*, 1582−1588.

(20) Comment, A.; van den Brandt, B.; Uffmann, K.; Kurdzesau, F.; Jannin, S.; Konter, J. A.; Hautle, P.; Wenckebach, W. T.; Gruetter, R.; van der Klink, J. J. Principles of Operation of a Dnp Prepolarizer Coupled to a Rodent Mri Scanner. *Appl. Magn. Reson.* **2008**, *34*, 313−319.

(21) Lide, D. R. *CRC Handbook of Chemistry and Physics*, 90th ed.; CRC Press: Boca Raton, FL, 2009.

(22) Comment, A.; van den Brandt, B.; Uffmann, K.; Kurdzesau, F.; Jannin, S.; Konter, J. A.; Hautle, P.; Wenckebach, W. T. H.; Gruetter, R.; van der Klink, J. J. Design and Performance of a Dnp Prepolarizer Coupled to a Rodent Mri Scanner. *Concepts Magn. Reson., Part B* **2007**, *31B*, 255−269.

DOI: 10.1021/acs.jpcc.5b07315
J. Phys. Chem. C 2015, 119, 22632−22639

(23) Stoll, S.; Schweiger, A.; Easyspin, A. Comprehensive Software Package for Spectral Simulation and Analysis in Epr. *J. Magn. Reson.* **2006**, *178*, 42−55.
(24) Abragam, A. *Principles of Nuclear Magnetism*; Oxford University Press: New York, 1961.
(25) Balzan, R.; Mishkovsky, M.; Solomon, Y.; van Heeswijk, R. B.; Gruetter, R.; Eliav, U.; Navon, G.; Comment, A. Hyperpolarized Li-6 as a Probe for Hemoglobin Oxygenation Level. *Contrast Media Mol. Imaging* **2015**, DOI: 10.1002/cmmi.1656.
(26) Borghini, M.; Udo, F. Dynamic Polarization of C-13 Nuclei in 1-Butanol. *Phys. Lett. A* **1973**, *43*, 93−94.
(27) Bowen, S.; Hilty, C. Rapid Sample Injection for Hyperpolarized Nmr Spectroscopy. *Phys. Chem. Chem. Phys.* **2010**, *12*, 5766−5770.
(28) Milani, J.; Vuichoud, B.; Bornet, A.; Mieville, P.; Mottier, R.; Jannin, S.; Bodenhausen, G. A Magnetic Tunnel to Shelter Hyperpolarized Fluids. *Rev. Sci. Instrum.* **2015**, *86*, 024101 1−8.

DOI: 10.1021/acs.jpcc.5b07315
J. Phys. Chem. C 2015, 119, 22632−22639